COMITATO NAZIONALE PER L'ENERGIA NUCLEARE
Laboratori Nazionali di Frascati

LNF-72/18
28 Febbraio 1972

R. Del Fabbro, G. Matone and V. Pocci: A SIMPLE ANALYSER FOR ELECTRON SCATTERING EXPERIMENTS ON NUCLEI. -

Servizio Documentazione
dei Laboratori Nazionali di Frascati del CNEN
Casella Postale 70 - Frascati (Roma)

Laboratori Nazionali di Frascati del CNEN
Servizio Documentazione

LNF-72/18
28 Febbraio 1972

R. Del Fabbro, G. Matone and V. Pocci: A SIMPLE ANALYSER FOR ELECTRON SCATTERING EXPERIMENTS ON NUCLEI. -

1. INTRODUCTION. -

In this note we propose a very simple magnetic device for the detection of scattered electrons at very small angles in electron scattering experiments on nuclei at high energy.

The present method allows for the measurement of angles and momenta of the scattered electrons and, at same time, bend of the incoming electron beam.

The widening effects on the angular and momentum resolution are essentially due to electron beam emittance, the multiple scattering in the target and the spatial indetermination of the detected trajectories. The contributions of this effect have been extensively investigated with a Monte Carlo method.

The resulting angular and momentum resolution becomes $\sim \pm 0.2^{o}$ and $\sim \pm 2\%$ respectively.

2. - MAGNETIC BOUNDARY SHAPE. -

We consider an electron of different energy point-like source, placed in a region of a static magnetic field. We refer to an orthogonal system of coordinates axes, where the origin is in the electron source and the x and z axis are oriented along the initial particles momenta and the magnetic field direction respectively.

We remark that if the boundary of the magnetic region follows the curve

(1) $$\frac{x}{y} = \left(\frac{d+y}{d-y}\right)^{1/2}$$

then the electron trajectory emerging from the magnetic region will be directly outgoing from a point-like virtual source in the position P(0, -d, 0). (See Fig. 1).

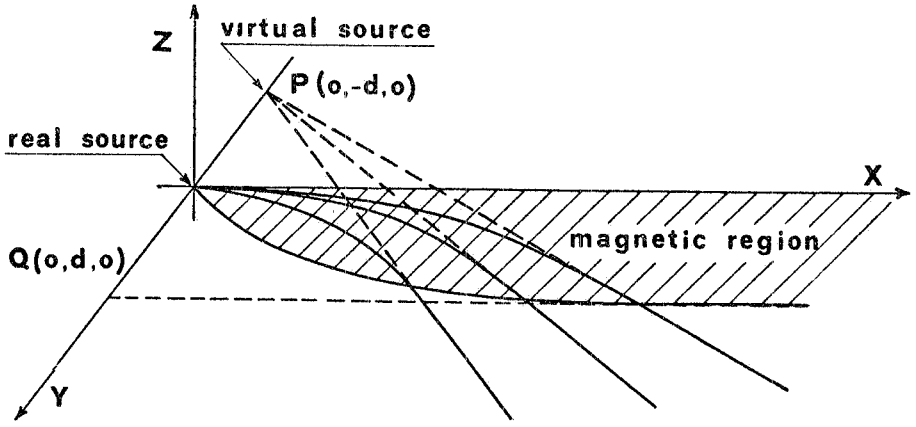

FIG. 1 - The magnetic field region $B=B_z$ and its optical properties are shown.

This result is exact and valid in the hypothesis of a fringing field sharp cutoff. However we shall consider only the electrons which cross the magnetic boundary on the points where $x \gg d$; indeed this limitation allows the use of the corresponding simple asymptote $y = d$ instead of the relation (1).

3. - ANGLE AND MOMENTUM ANALYSIS. -

If we consider electrons at fixed energy emitted in a finite cone solid angle around the x direction, with simple geometrical considerations, we can get the following two formulas :

(2) $$\cos\beta = \cos\gamma - 2\sin^2 \alpha/2$$

(3) $$\cos\gamma = (R-d)/R$$

where:

α - is the initial projected angle in the (x, y) horizontal plane;
$\gamma, (\beta)$ - is the final projected angle in the (x, y) horizontal plane of the central trajectory (generic trajectory of the cone) outgoing from the magnetic region;
R - is the curvature radius.

Table I shows the order of magnitude of the main geometrical characteristics of a possible electron analyser.

TABLE I

Length of the magnetic along the scattered electron direction.....	2.-3. m
transvers length of the magnet.....	.15-.25 m
total angular deviation.....	10^{o}-15^{o}
half-angular magnitude (α) of the emitted electron cone.....	1^{o}-2^{o}
curvature radius.....	$\sim$ 10. m

From the set of values shown in Table I, electrons with the same energy, but with different α angle, go out practically parallel, as is shown by the following relation deduced from the equation (2):

$$\frac{\beta-\gamma}{\gamma} \sim 1/2\left(\frac{\sin \alpha/2}{\sin \gamma/2}\right)^2 \sim 10^{-2}$$

Thanks to this optic property, the curvature radius, and of course the momentum, can be simply evaluated from the equation (3) measuring the outgoing angle.

Moreover an aitractive aspect of this set-up is the possibility of measuring the angle α with a good angular resolution. Indeed, as shown in Appendix 1, for electrons of the same energy, the distance h from the central projected trajectory to a generic one, is expressed by the following approximate relation:

$$h_{+-} \simeq R \sin\gamma \left| \sin\alpha \right| \pm 2 \sin^2 \alpha/2 \left(R\cos\gamma - \frac{s}{\sin\gamma}\right) \tag{4}$$

where s is the distance from the magnet to the point where we consider the displacement between the trajectories, (see Fig. 2) and h_{+-} is labelled with two signs corresponding to the two possible values of $\pm|\alpha|$.

If s is chosen of the order of $R\cos\gamma \sin\gamma$, because of the smallness of the angle α, the relation (4) becomes:

(5) $$h_{+-} \simeq d \frac{\sin \gamma}{1-\cos \gamma} |\alpha|$$

We observe that a measure of the angle α needs a suitable energy calibration of the whole system including the magnet and the particle detectors.

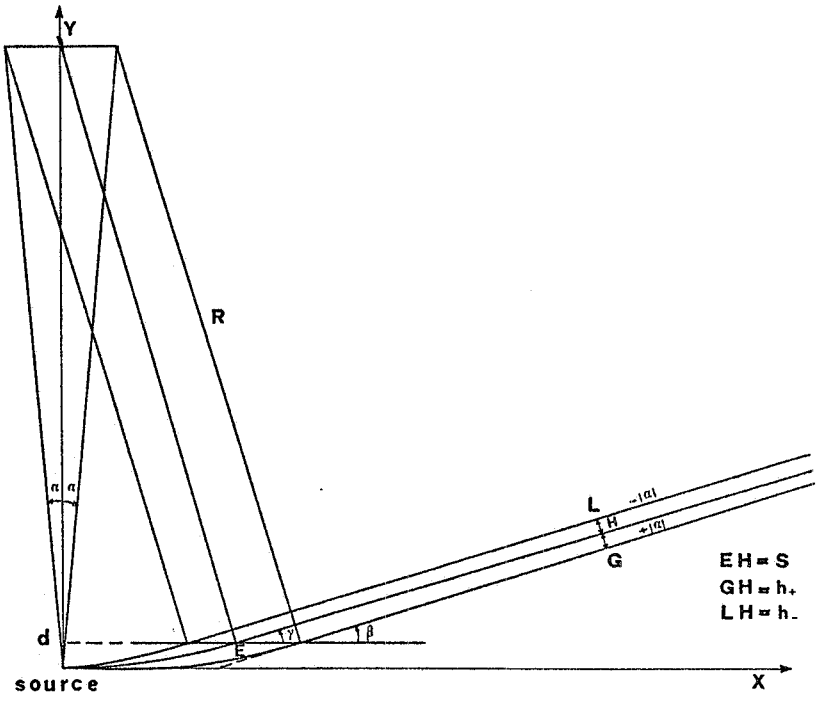

FIG. 2 - Projection of two symmetrical trajectories in the (x, y) plane for monocromatic electrons. The angles and the distances do not exhibit the true proportions for illustrative purpose.

4. - FRINGING FIELD EFFECTS. -

It is necessary to show that all these considerations are still valid even if we take into account the fringing field effects.

In order to simplify the study of electron trajectories at the edge of the magnet, we assume a strip of width ℓ, where the magnetic fields has a linear behaviour. As it is shown in reference (1), it is possible to obtain this condition by means of standard quadrupole arrangement of the magnet poles.

Appendix 2 summarizes the results of our calculation on the motion of electrons in a linear varying magnetic field.

So we have investigated the behaviour of the output angle ε' versus the input angle ε for different values of width ℓ (See figure 3).

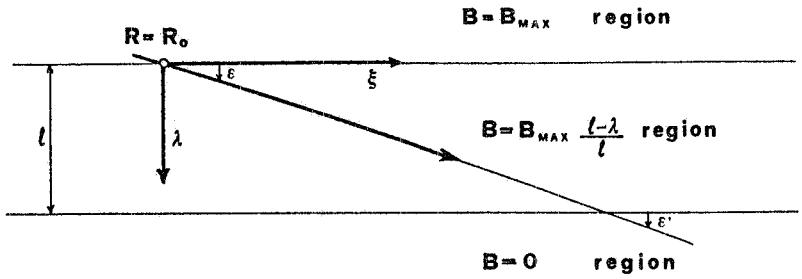

FIG. 3 - Outline of the fringing field strip showing the magnetic field map.

We want to remark that, if we limit ourselves to the following ε and l ranges :

$$5^{o} \leq \varepsilon \leq 20^{o} \qquad\qquad 0 \leq l \leq 20 \text{ cm},$$

the angle ε' results linear in the ε and l parameters.

In conclusion, with a linear arrangement of the fringing magnetic field and hence taking into account its additional contribution, our previous deductions remain valid.

5. - ANGLE AND MOMENTUM RESOLUTION. -

In order to study the angle and momentum resolutions of the analyser, it is useful to fix its geometrical parameters as indicated in Table II.

TABLE II

Magnetic length	2	m
γ	12^{o}	
d	15	cm
l	10	cm
s	1.7	m
α	1^{o}	
R	10	m

Of course the same optical configurations are relative to an arbitrary energy of the scattered electrons by means of a suitable magnetic field intensity (The range available is seen in the Fig. 4).

The emittance of incoming beam, the radiation length of the target and the spatial resolution of the electron detecting apparatus are considered as free parameters in a Monte Carlo calculation.

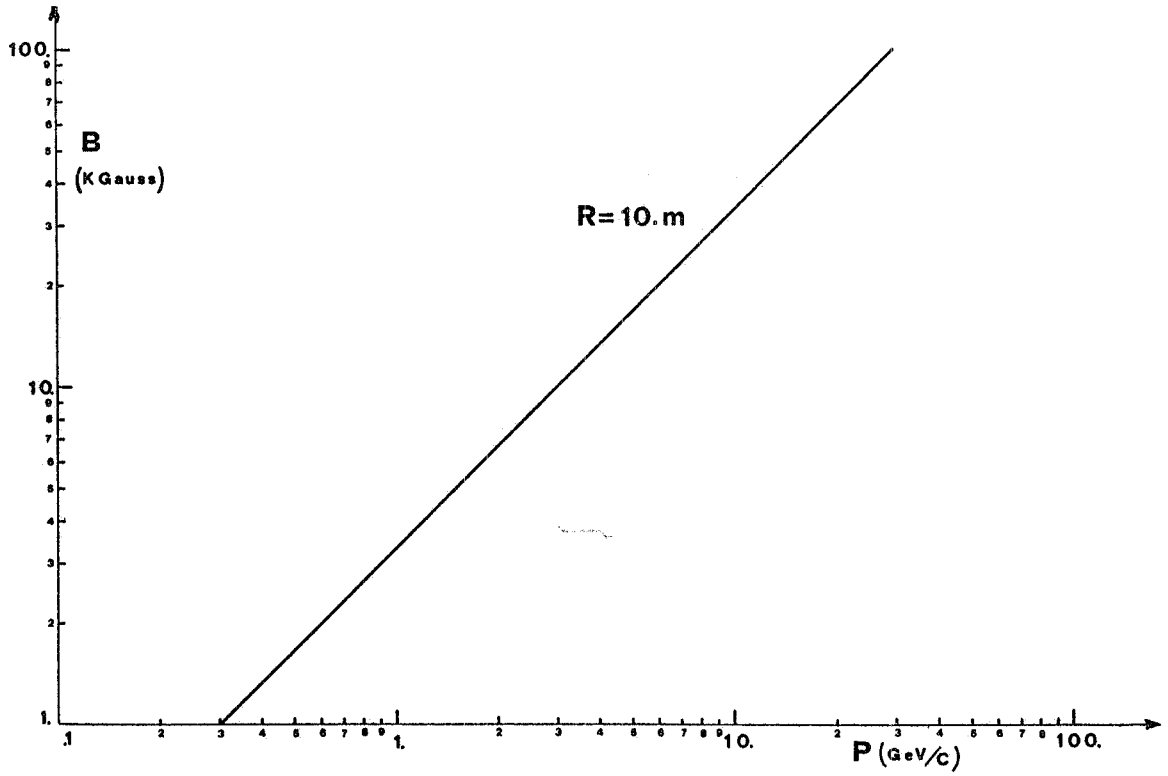

FIG. 4 - Momentum range of the scattered electron versus the intensity of the magnetic field available to electron analyser. The curve corresponds to a central curvature radius of 10 m.

The solid angle accepted results about 2 msterad ($\pm$ 1° in horizontal and $\pm$ 2° in vertical direction), and the momentum acceptance is considered to be $\sim \pm$ 20 %. So we note that by the relation we have from (3): $|\Delta\gamma/\gamma| \sim 1/2\,|\Delta p/p|$, the range of the angle γ is limited to $\pm$ 1°.

The final results shown in the figures 5 and 6 concern the shape of the standard deviation relative to the angle and momentum resolution versus the widening parameters, which are presented superimposed in many dispositions.

The standard deviations of the resolutions obtained from the Monte Carlo are drawn versus the spatial resolution of the detected electrons. Two or three curves are considered corresponding to different values of the multiple scattering angle. The angles of deviation due to a finite emittance of the beam are generally smaller and they are not been considered. However the spatial intensity of the spot assumed gaussian is directly connected with the emittance; we have considered different values of its standard deviation r. We note that normal values of r are 1 or 2 mm.

Considering a standard value of the emittance and of the target thickness, we find that the angular resolution and the momentum resolution of 2 GeV/c scattered electrons (B = 6.7 KG) are better than $\pm$ 0.2° and $\pm$ 2 % respectively.

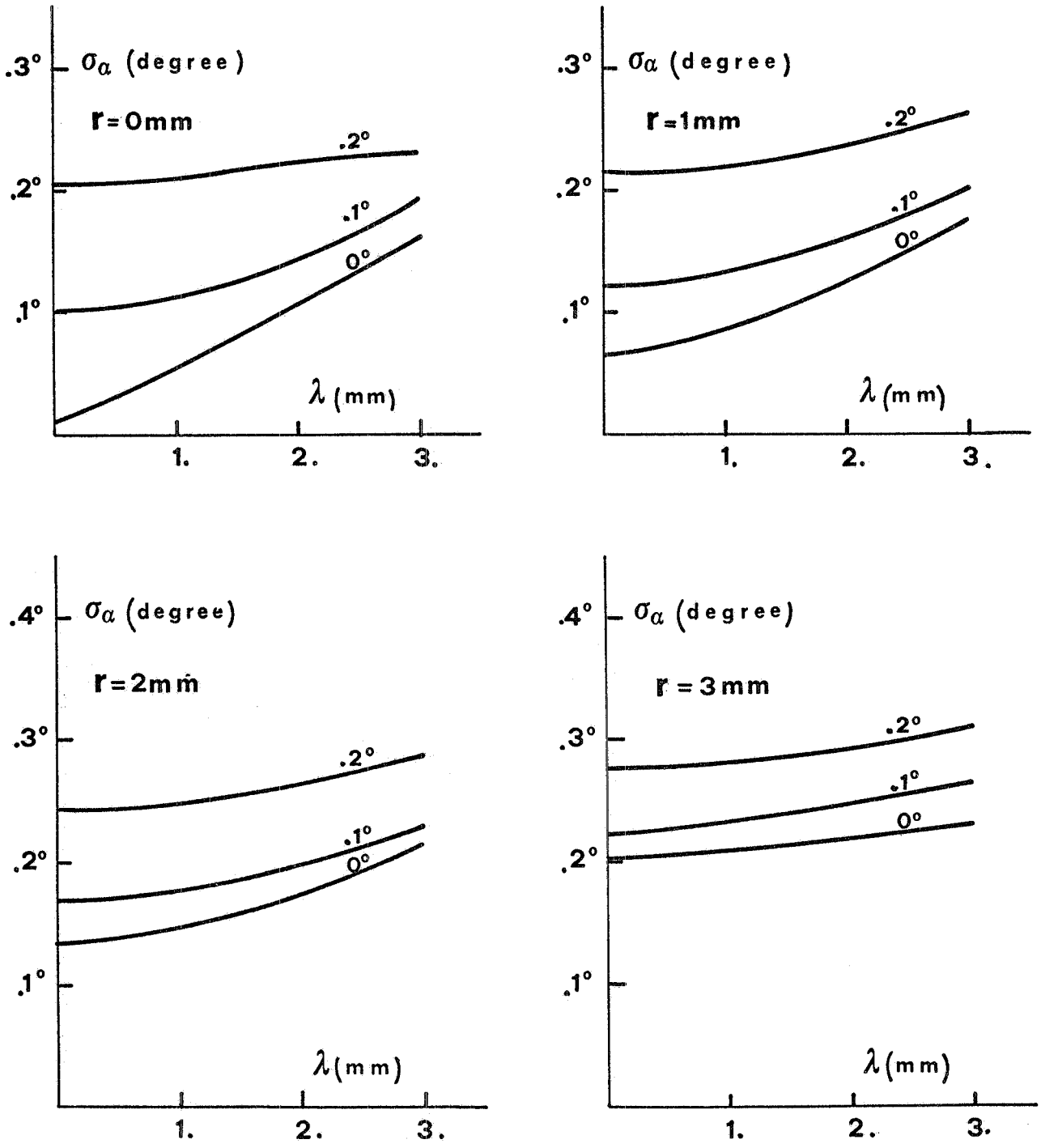

FIG. 5 - Standard deviation plot of the Monte Carlo angular resolutions versus the spatial resolution of the detected trajectories. The beam spot is assumed to have a gaussian spatial intensity distribution and r is its standard deviation. Different curves correspond to scattering multiple angle of 0^{o}, $.1^{o}$ and $.2^{o}$ respectively.

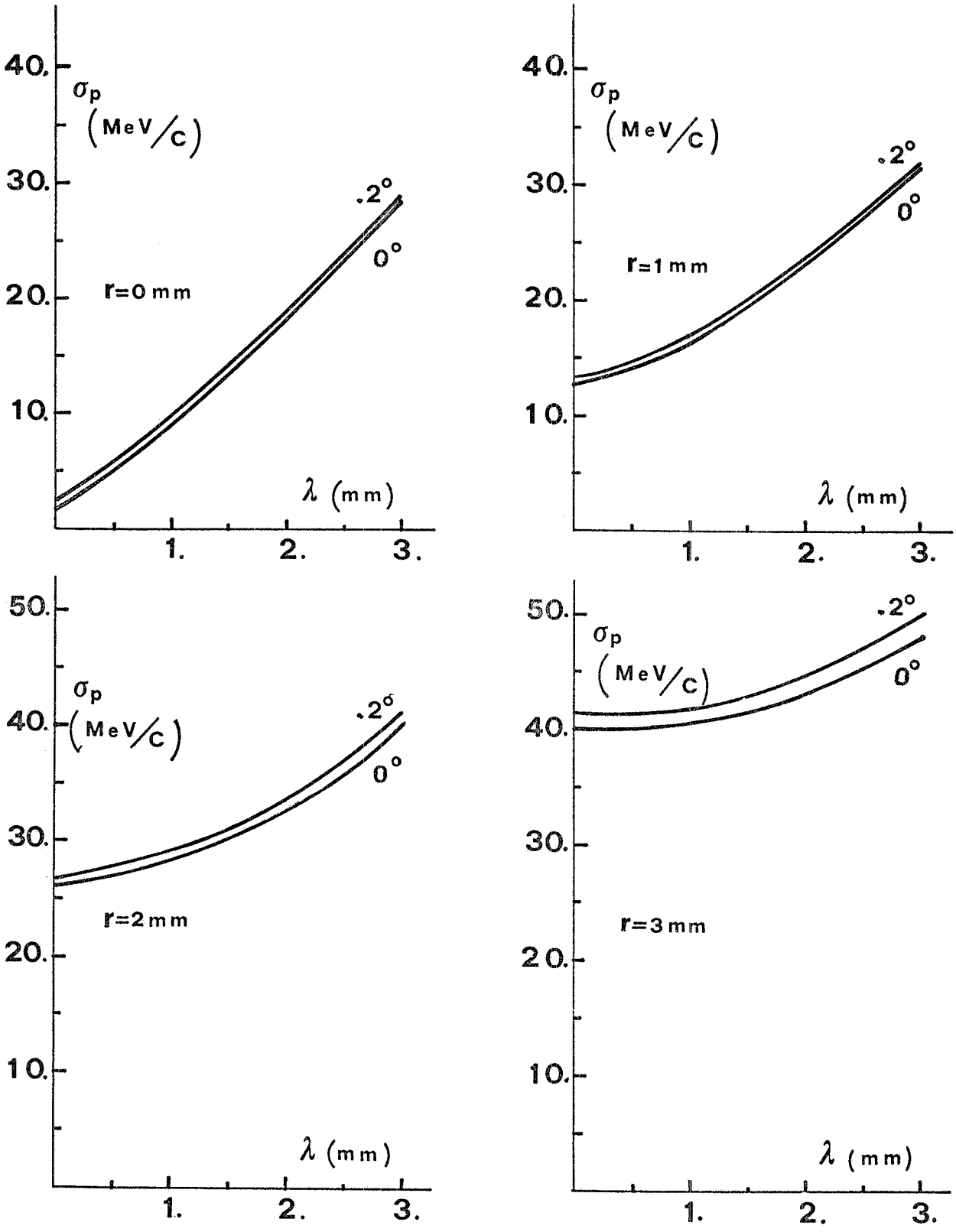

FIG. 6 - Standard deviation plots of the Monte Carlo momentum resolution versus the spatial resolution of 2 GeV/c electron momentum. The beam spot is assumed to have gaussian spatial distribution and r is its standard deviation. Different curves correspond to multiple scattering angle of 0^{o} and $.2^{o}$ respectively.

In the case of electron experiments on high Z elements, the dimension of the target along the x direction is always considered negligible.

APPENDIX I. -

To find the displacement expression of the projected trajectories relative to electrons of the same energy, the distances h_+ and h_- of trajectories (corresponding to $\alpha = \pm |\alpha|$) symmetrical to the central one are considered.

The set up is shown in figure 2; it is straightforward to verify that the symmetrical trajectories are parallel and displaced of $h_+ + h_- = 2R \sin\alpha \sin\beta$.

The deduction of the difference $h_+ - h_-$ is rather tedious, because it depends on the point of the central trajectory where the displacement is considered.

Nevertheless, if we refer to the point E of figure 2, it can be shown that $h_+ - h_- = 2R \sin^2\alpha/2 \cos\beta K$, where

$$K = \sec(\beta-\gamma)\left(1 + \frac{\cos\gamma}{\cos\beta}\right)/\left(1 + \frac{\sin\gamma}{\sin\beta}\right) \simeq 1$$

so the expression of h_{+-} becomes

$$h_{+-} \simeq R \sin\alpha \sin\beta \pm 2R \sin^2\alpha/2 \cos\beta \ .$$

We can write a more general expression of h_{+-}; namely when we consider the displacement in a generic point H, we obtain:

$$h_{+-} \simeq R \sin\alpha \sin\beta \pm \left[2R \sin^2\alpha/2 - s\,\mathrm{tg}(\beta-\gamma)\right]$$

where $s = \overline{EH}$.

Finally let us find a significant form of the last expression; indeed by the approximation of $\sin[(\beta/2) + (\gamma/2)]$ to $\sin\gamma$ we have that $\mathrm{tg}(\beta-\gamma) = (2\sin^2\alpha/2)/(\sin\gamma)$ and after some elaborations we can get the following expression:

$$h_{+-} \simeq R \sin\alpha \sin\gamma \left[1+2\left(\frac{\sin\alpha/2}{\sin\gamma/2}\right)^2\right] \pm 2\sin^2\alpha/2\left(R\cos\gamma - \frac{s}{\sin\gamma}\right) + 0(\alpha^4)$$

APPENDIX II. -

Let us consider the problem of the electron motion in a linear decreasing magnetic field as

$$B = B_{MAX}\,\frac{1-\lambda}{l}$$

where λ is the generic coordinate.

The projected equations of motion are reducible to the system of two differential equations of the kind :

$$\ddot{y} = \dot{x}\, y \; ; \qquad \ddot{x} = -\dot{y}\, y \; ;$$

the solutions of this system can be expressed in terms of elliptic integral of the first kind

$$F(\alpha, \varphi) = \int_{\cos\varphi}^{1} \frac{d\omega}{(1-\omega^2)^{1/2}\,(\cos^2\alpha + \sin^2\alpha\ \omega^2)^{1/2}}$$

and they have the following form in the system of coordinates axes shown in figure 4 :

$$\xi(t) = v t \cos\varepsilon - \frac{v}{R_o}\int_0^{\tau} \lambda(\tau)\, d\tau \; ; \qquad t = k\cos\alpha\left[F(\alpha, \varphi_o) - F(\alpha, \varphi)\right]$$

where v is the velocity of the electron, $R_o = d/(1 - \cos\varepsilon)$ is the initial curvature radius and t the time coordinate ; moreover the other introduced symbols are defined :

$$k = 2R_o/v\,G_+ \, , \qquad \operatorname{tg}\alpha = G_+/G_- \, , \qquad \cos\varphi = (1 - \lambda)/G_-1 \, ,$$

where $G_{\pm} = \left[\frac{2R_o}{1}(1 \pm \cos\varepsilon) \mp 1\right]^{1/2}$.

These solutions with the initial conditions allow for obtaining a complete description of the electron motion ; therefore by calculation the resulting behaviour of ε' within respect of ε and 1 is linear inside the limits of range, we have shown in the text.

REFERENCE. -

(1) - A quadrupolar magnetic fringing field can be obtained (e. g. "High energy optics" of K. G. Steffen, Interscience publishers J. Wiley & Sons, New York) by changing the plane poles of the magnet with hyperbolic surfaces at the edge and by disposing an high μ-plane in the equipotential quadrupole plane. The linear behaviour of the field is slightly modified by the hole for the electron output.